High-efficiency solenoid coil structure for induction heating of cylindrical heating object

Daiki Miyake, Kazuhiro Umetani, Shota Kawahara, Masataka Ishihara, and Eiji Hiraki
Graduate school of natural science and technology,
Okayama University,
Okayama, Japan

Published in: 2022 IEEE 31st International Symposium on Industrial Electronics (ISIE)

DOI: 10.1109/ISIE51582.2022.9831459

High-Efficiency Solenoid Coil Structure for Induction Heating of Cylindrical Heating Object

Daiki Miyake
Graduate school of natural science and technology
Okayama University
Okayama, Japan
p47s66ad@s.okayama-u.ac.jp

Kazuhiro Umetani
Graduate school of natural science and technology
Okayama University
Okayama, Japan
umetani@okayama-u.ac.jp

Shota Kawahara
Graduate school of natural science and technology
Okayama Univesity
Okayama, Japan
pnb577k8@s.okayama-u.ac.jp

Masataka Ishihara
Graduate school of natural science and technology
Okayama University
Okayama, Japan
masataka.ishihara@okayama-u.ac.jp

Eiji Hiraki
Graduate school of natural science and technology
Okayama University
Okayama, Japan
hiraki@okayama-u.ac.jp

***Abstract*— The solenoid coil is a typical heating coil structure for induction heating of cylindrical heating objects. Conventionally, a bare solenoid coil without any soft-magnetic core has been commonly utilized. However, this conventional structure suffers from worse heating efficiency caused by the large coil copper loss and the low magnetic field induction at the heating object. This paper addresses these difficulties by proposing a novel heating coil structure. In addition to the solenoid coil, the proposed heating coils structure further incorporates the soft-magnetic cores that cover the outer coil periphery and the coil opening edges. These additional cores can reduce the local intense magnetic field around the coil, thus mitigating the eddy current induction inside the wire to reduce the copper loss, and also can increase the magnetic field inside the heating object, thus increasing the heat generation. The simulation was carried out to test the effectiveness of the proposed heating coil structure. The results inferred the reduction of the coil copper loss by 25% and the increase in the heat generation in the heating object by 53%, both of which suggest the promising features of the proposed heating coil structure for heating the cylindrical magnetic material. The heating operation of the proposed heating coil structure was tested by the experiment, although the current prototype was found to have larger power loss than expected from the simulation. The reason may lie in unintended eddy current generation of the metal case of the heating coil, which will be addressed in future work.**

Keywords*— *copper loss, eddy current, induction heating, magnetic field, solenoid coil.

I. Introduction

Induction heating is a safe and convenient heating technology for conductive and magnetic materials by utilizing electric power. The induction heating can heat the material without combustion. Therefore, the induction heating is free from the safety equipment against the risk of conflagration, oxygen consumption, and carbon dioxide generation, thus enabling this heating technology to be applied to the various environment where the safety equipment is difficult to be installed. Furthermore, the heat generation can be finely controlled by utilizing the electric circuit, enabling induction heating to be applied to various applications where accurate and fast control of the temperature is required. Owing to these benefits, induction heating finds various applications in the industry [1]-[4] and home appliances[5]-[9].

The induction heating can heat the various shape of the heating object. However, one of the most typical shapes of the heating object is the cylinder. For example, induction heating is widely utilized to heat the billets of metal [10][11], e.g. steel, aluminum, light alloy, etc. Induction heating is also known as a popular method for welding metal pipes [12][13]. Furthermore, induction heating can be utilized to heat the cylindrical catalyst with thin holes through which the chemical reactants flow. For example, [14][15] investigate the NOx elimination system for combustion engines by finely controlling the temperature of cylindrical catalyst of magnetic material using induction heating.

Figure 1 depicts a typical induction heating system with a conventional heating coil structure for cylindrical conductive or magnetic material. This system comprises a solenoid coil wound around the heating object. The solenoid coil, which we denote hereafter as the heating coil, is connected in series with the resonant capacitor and the transformer secondary winding. The transformer primary winding is connected to the high-frequency

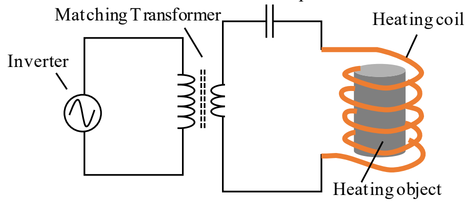

Fig. 1. Induction heating system with conventional heating coil structure.

inverter, which outputs the high-frequency ac voltage and induces the ac current in the heating coil.

The frequency of the ac voltage is adjusted to the resonant frequency of the heating coil and the resonant capacitor. Therefore, the ac voltage can excite the resonance and induce large resonance current in the heating coil. This current generates intense magnetic field around the heating coil. Therefore, exposed to the intense magnetic field, the heating object generates the heat inside itself caused by the ohmic loss of the eddy current or the magnetic loss in the heating object, without contact with the heating coil.

As can be seen in Fig. 1, the conventional induction heating coil structure has a simple structure comprising only a solenoid coil typically made of the round- or square-shaped wire. However, this conventional heating coil structure tends to exhibit bad heating efficiency, i.e. the ratio of the heat generated in the heating object to the input electric power to the coil, as discussed in the subsequent section. This drawback of the conventional heating coil structure requires excessive electric power for the ac power supply and the strong cooling environment for the heating coil, which needs to be overcome for further spread of the induction heating technology.

The purpose of this paper is to propose a novel heating coil structure that can improve heating efficiency. As analyzed in the subsequent section in detail, the reason for this bad efficiency lies in small magnetic field induction in the heating object and large copper loss inside the heating coil. To overcome these difficulties, the proposed heating coil structure adds a magnetic structure for increasing the magnetic field in the heating object and reducing the copper loss, which were proven by the simulation on the heating of a cylindrical magnetic material.

The remainder of this paper comprises 4 sections. Section II analyses the conventional heating coil structure and elucidates the mechanism of its drawbacks. Section III proposes a novel heating structure and theoretically discusses how this structure can mitigate these drawbacks. Then, section IV reports the simulation to evaluate the principles of the proposed heating coil structure. Section V reports an experiment to test the performance of the proposed heating coil structure. Finally, section VI gives the conclusions.

II. Problems of Conventional Coil Structure

The conventional heating coil structure shown in Fig. 1 suffers from the small magnetic field induction in the heating object and the large copper loss of the heating coil. This section theoretically discusses these problems by analyzing the magnetic field distribution around the heating coil. Hereafter, the heating object is assumed to be a non-conductive magnetic material with small permeability similar to the vacuum, as is in the simulation and the experiment, although a similar discussion stands also in the case where the heating object is conductive or has far greater permeability than the vacuum.

Firstly, the small magnetic field induction is originated from generating the magnetic field that does not contribute to the induction heating. According to Ampere's law, the integration of the magnetic field along a closed-loop line is identical to the sum of the current flowing through the loop. Therefore, the magnetic integration along the flux line circulating the winding,

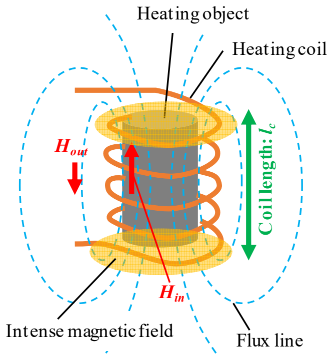

Fig. 2. Magnetic fux lines around conventional heating coil structure.

as illustrated in Fig. 2, is identical to the magnetomotive force of the winding. Let H_{in} and H_{out} be the typical magnetic field on the flux line inside and outside the conventional heating coil structure, the following relation can be obtained by neglecting the magnetic field integration at the coil edge:

$$H_{in}l_c + H_{out}l_c \approx Ni_{ac}, \tag{1}$$

where l_c is the length of the heating coil, N is the number of turns, i_{ac} is the ac current of the heating coil.

It is worth noticing that H_{in} is the magnetic field applied to the heating object. Therefore, H_{in} should be as great as possible for effective heat generation under the limited ac current of the heating coil. For this purpose, H_{out} should be as small as possible according to (1). In the conventional structure, however, the outer periphery of the heating coil is covered by a non-magnetic material. Consequently, H_{out} tends to be large due to the small permeability, which results in the small magnetic field induction inside the heating coil, i.e. H_{in}, and reduces the heat generation.

Secondly, the large copper loss of the heating coil is originated from two reasons. One is that the round- or square-shaped wire is used for the heating coil, and the other is that the local intense magnetic field is generated around the wire of the heating coil. The former reason is straightforward. The wire thickness of the round- or square-shaped wire must be smaller than the thickness of the heating coil. However, in many solenoidal heating coils, the coil thickness is far smaller than the coil length and the number of turns tends to be small in high-frequency induction heating. As a result, the surface area of the wire is restricted by the mechanical requirement of the heating coil thickness although the conventional heating coil structure tends to contain much vacant space between adjacent turns.

According to the electromagnetism, the high-frequency ac current in the wire is confined at the wire surface if the wire thickness is far greater than the skin depth δ [16] defined as

$$\delta = \sqrt{2\rho/\omega\mu} \tag{2}$$

where ρ is the resistivity of the wire material, ω is the angular frequency of the ac current, and μ is the permeability of the wire material. In high-frequency induction heating, the wire thickness is generally far greater than the skin depth. Therefore, a small

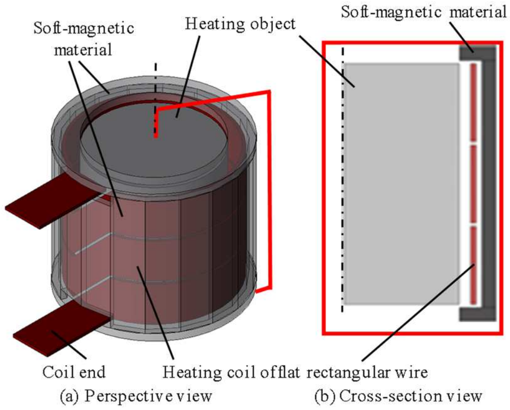

Fig. 3. Proposed heating coil structure.

surface area of the wire results in a small cross-section area for the ac current flow, thus generating large copper loss.

Regarding the latter reason, we should remind that the copper loss of the heating coil is greatly dependent on the ac magnetic field distribution around the wire of the coil. As discussed in [17], the surface current crossing the unit length of the surface is identical to the surface magnetic field of the wire, if the wire thickness is far greater than the skin depth. If the ac current of the wire is uniformly distributed in the whole wire surface, the surface magnetic field must be $H_s=I_{ac}/l_s$, where l_s is the length of the wire cross-section periphery. Therefore, the surface magnetic field greater than I_{ac}/l_s must result in the inhomogeneity of the ac current distribution, indicating the eddy current and therefore should be reduced to reduce the copper loss.

The magnetic field at the wire surface of the heating coil tends to be large, particularly near the opening edges of the heating coil in the conventional structure. According to electromagnetism, the bending flux line generates the inhomogeneity of the magnetic flux density: the inner side of the flux line has greater magnetic flux density than the outer side [18][19]. This inhomogeneity tends to be prominent where the flux line curves sharply. In the conventional structure, the magnetic flux lines curve sharply at the coil opening edges, where the large magnetic flux density occurs. Furthermore, because the openings are covered by non-magnetic materials, the large magnetic flux density results in intense magnetic field due to the low permeability. Consequently, large eddy current tends to occur at the coil edge, thus causing large copper loss.

III. Proposed Heating Coil Structure

This section proposes a novel heating structure to overcome the aforementioned problems of the conventional heating coil structure. Figure 3 illustrates the proposed heating coil structure. Compared with the conventional heating coil structure, the proposed structure incorporates three prominent features: 1. A soft-magnetic material is disposed to cover the outer periphery of the coil, 2. The heating coil is made of a flat rectangular wire, 3. A soft-magnetic material is disposed of on the coil edges.

As discussed in the previous section, the magnetic field outside the heating coil should be small as possible to obtain great magnetic field inside the heating coil. For this purpose, the soft-magnetic material is disposed on the backside of the heating coil to provide the flux path for the ac magnetic flux generated by the heating coil. The soft-magnetic material can reduce the magnetic field owing to its high permeability. By entirely covering the outer periphery of the heating coil, the magnetic field H_{out} can be neglected, to maximize the magnetic field H_{in}, thus contributing to increasing the heat generation and improving the heating efficiency.

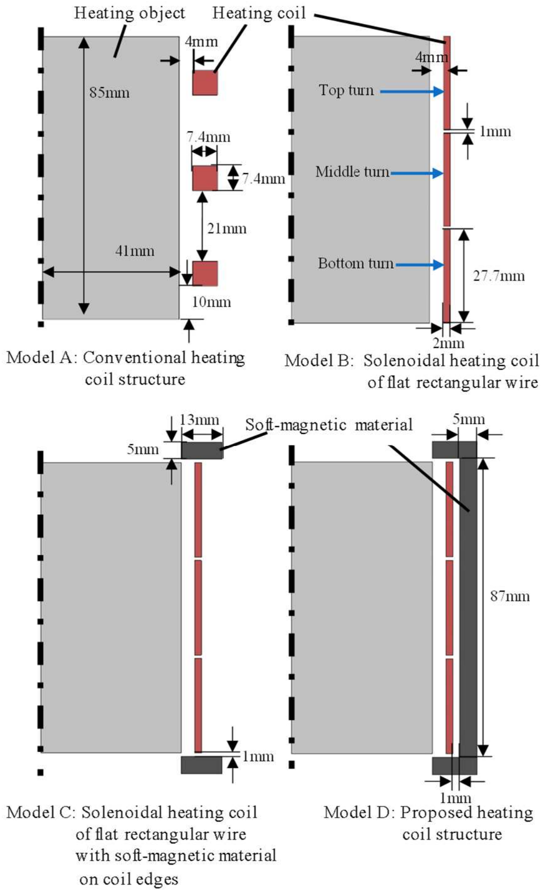

Fig. 4. Cross-section view of simuation models.

According to the previous section, the round- or square-shaped wire of the conventional heating coil caused the limited wire surface area, which was one of the reasons for large copper loss. This problem was addressed in the proposed structure by adopting a flat rectangular wire. The flat rectangular wire should be designed to minimize the vacant space between the adjacent turns. This can maximize the wire surface and reduce the copper loss by providing large cross-section area for the ac current.

Regarding the last reason for the large copper loss in the conventional structure, the proposed structure adds a soft-magnetic material to cover both the top and bottom edges of the heating coils. In the solenoidal coil, the opening edges of the heating coil experience great magnetic flux concentration due to the sharply bending flux lines. The proposed structure provides the flux path with high permeability to these flux lines to reduce the magnetic field at the coil edges.

As seen above, the proposed structure can solve all the problems listed in the previous section. Consequently, the proposed heating coil structure can be expected to improve the heating efficiency by increasing the magnetic field induction in the heating object and suppressing copper loss generation at the heating coil.

IV. Simulation

The electromagnetic simulation was carried out to evaluate the principles of the proposed heating coil structure. In this simulation, the four heating coil structures, as shown in Fig. 4, were compared to test the effectiveness of the proposed structure: A. the conventional heating coil structure of square-shaped wire; B. the solenoidal heating coil of flat rectangular wire; C. the solenoidal heating coil of flat rectangular wire with the soft-magnetic material covering the top and bottom coil edges; D. the proposed coil structure, which further incorporates the soft-magnetic material covering the outer periphery of the heating coil.

Table I shows the specifications of the simulation models. In this simulation, all the heating coils were designed to have three turns of the wire with the same cross-section area. Therefore, these heating coils had the same dc resistance. These heating coils carried the ac current of 333 Arms at the frequency of 500 kHz. The heating object was a non-conductive magnetic material with a permeability of 1.1. In this simulation, the heating object is lossless. However, the heat generation was estimated by calculating the square value of the magnetic field intensity averaged over the heating object. (The heat generation was approximated to be proportional to the square of the magnetic field intensity.) The conductivity of the wire was set at that of the copper at 25 °C. The soft-magnetic material employed in models B-D was assumed to have the same B-H characteristic as PC40 (TDK Corp.) with a resistivity of 6.5 Ω·m.

Figure 5 shows the simulation results of the magnetic field in the heating object. The distribution of the magnetic field intensity exhibited great inhomogeneity inside the heating object in the conventional heating coil structure (model A). This is caused by the concentrated current distribution of the heating coil due to the large vacant space between the adjacent turns. However, the overall magnetic field in the heating object was almost the same among models A-C, although a prominent increase of the magnetic field was observed in model D, which incorporates the soft-magnetic material covering the outer periphery of the heating coil. On the other hand, the magnetic field intensity outside the heating coil was greatly reduced in model D in comparison with models A-C. These features were consistent with the analytical discussion of the previous section owing to the soft-magnetic material covering the outer periphery of the coil.

Figure 6 shows the comparison results of the squared magnetic field intensity averaged over the heating object. As can be seen in the figure, the squared magnetic field intensity was almost the same among models A-C, although a prominent improvement was found in model D by 53% in comparison with model A, as is expected from the analytical discussion.

Next, the copper loss of the heating coils was evaluated. Figure 7 shows the comparison results of the power loss of the heating coil among the simulation models. Figure 8 shows the close-up view of the wire current distribution where the prominent difference was found. As can be seen in Fig. 7, the power loss is mainly caused by the copper loss in the wire rather than the iron loss in the soft-magnetic material. Model B reduced the copper loss of all the turns compared to model A. According to Fig. 8(a), the current density is confined to the wire surface in all simulation models. However, the current density at the wire surface of model B is much smaller than that of model A. This can be consistently interpreted as the result of the increase of the wire surface area by the flat rectangular wire.

Figure 7 also exhibited that model C further reduced the copper loss compared to model B. The reduction effect was mainly found in the top and bottom turns, which face the coil edges. Figure 8(b) plots the current distribution of models B and C at the coil edges. As can be seen in this figure, model B

TABLE I. Simulation Settings

Operating frequency	500kHz
AC current of heating coil	333Arms
Number of turns	3
Soft-magnet material	TDK Corp. PC40
Relative permeability of heating object	1.1

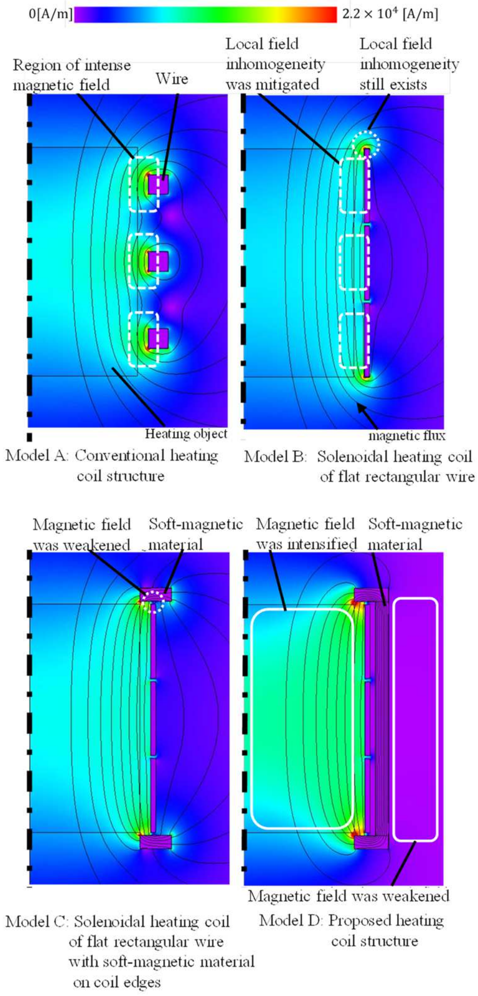

Fig. 5. Simulated magnetic field distribution.

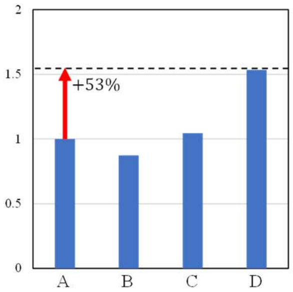

Fig. 6. Squared magnetic field intensity averaged over heating object normalized by that of model A.

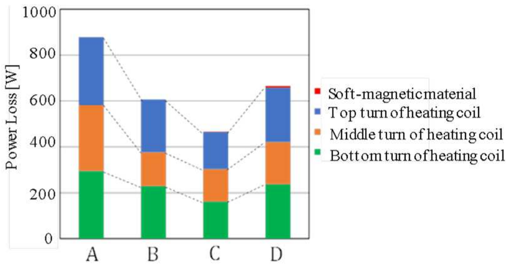

Fig. 7. Simulated power loss breakdown of heating coil structure.

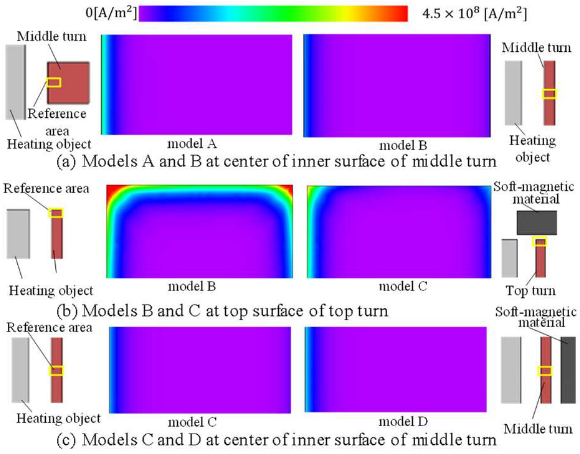

Fig. 8. Simulated current density distribution in heating coil wire cross-section.

exhibited the current concentration at the coil edge, whereas model C solved the concentration using the soft-magnetic material disposed at the coil edge. This is also consistent with the analytical discussion in sections II and III. Therefore, the simulation supported the effectiveness of both of the two features of the proposed structure for reducing the copper loss, i.e. the flat rectangular wire and the soft-magnetic material covering the top and bottom coil edges.

Certainly, the copper loss increased in the proposed structure, i.e. model D, compared to model C. However, this increase is the natural consequence of the increase in the magnetic field inside the heating coil. As discussed in section II, the current crossing the unit length of the wire surface equals the magnetic field at the wire surface. Therefore, the current density is increased in model D at the wire surface facing the inner side of the heating coil, as shown in Fig. 8(c), due to the magnetic field increase at the inner side of the heating coil, which is intended to increase the heat generation in the heating object. Nonetheless, the proposed structure reduced the copper loss approx. by 25% compared to the conventional structure thanks to the flat rectangular wire and the soft-magnetic material covering the coil edges.

Consequently, the simulation supported the appropriateness of the principles of the proposed heating coil structure. The simulation also suggested that the proposed structure can increase the heat generation with smaller copper loss, which is effective to improve the heating efficiency.

V. Experiment

An experiment was carried out to test the performance of the proposed heating coil structure. The structure of the experimental prototype of the proposed heating coil structure is the same as Fig. 3. The size of the wire and coil were designed to be identical to those used in the simulation.

Figure 9 shows the photographs of the experimental prototype. The heating coil has three turns. The thickness and width of the wire of the heating coil were 2 mm and 27 mm, respectively. The inner diameter of the heating coil was 90 mm. As can be seen in the simulation results, the majority of the ac current of the heating coil is confined to the inner surface within the skin depth. However, the thickness of the experimental heating coil was far greater than the skin depth at 400 kHz, which was set as the operating frequency of the inverter. In this sense, the thickness of the heating coil was far greater than necessary for providing the cross-section area for the ac current. The reason for this excessive thickness was to implement sufficient thermal capacitance to spread the heat and mitigate the local temperature rise due to the inhomogeneity of the heating coil loss generation.

The heating object was the cylindrical filter of a magnetic material, which is utilized to heat the airflow. The permeability of the heating object was estimated as 1.1. The height and inner diameter of the heating object were 85 mm and 82 mm, respectively. The materials used for the prototypes were listed in Table II. As this experiment is intended for heating the air flowing through the heating object, the metal duct tube was needed to form the airflow path through the heating object. Therefore, the whole heating coil including the heating object was packed in the stainless steel case and connected to the metal duct tube. These metals can reduce the heating efficiency due to the possible eddy current induction by the heating coil. Nonetheless, the non-magnetic material was chosen for the case to avoid the excessive induction of the eddy current.

This prototype of the heating coil was supplied with the ac current using the circuit system shown in Fig. 10. The heating coil was connected to the resonant capacitor and the transformer secondary winding. The capacitance of this resonant capacitor was 0.15 μF; the inductance and the ac resistance of the heating coil including the heating object were 0.96 μH and 160 mΩ, respectively, at the operating frequency of 400 kHz, which was close to the resonant frequency of the resonant capacitor and the heating coil. Then, the inverter was connected to the transformer primary winding to induce the ac current in the heating coil.

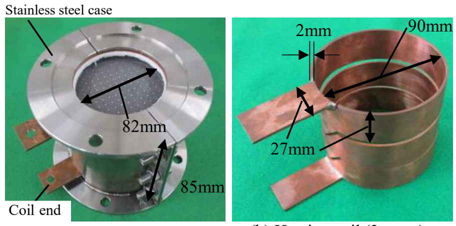

(a) Overall view (b) Heating coil (3 turns)

Fig. 9. Experimental circuit of proposed heating coil structure.

TABLE II. MATERIALS FOR PROTOTYPE

Heating coil	Copper
Soft-magnetic material	TDK Corp. PC40
Stainless steel case	SUS304

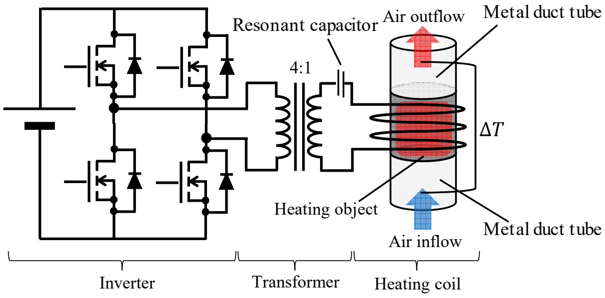

Fig. 10. Experimental circuit of proposed heating coil structure.

In this experiment, we evaluated the heat generation in the heating object as well as the copper loss of the heating coil. The heat generation of the heating object was estimated by measuring the amount of airflow per second and the temperature of the airflow before and after the air passed the heating object. If Q and ΔT denote the amount of the airflow per second at the inlet and the temperature difference between before and after the airflow passes the heating object, respectively, the heat generation per second P_{heat} can be estimated as

$$P_{heat} = Q\rho c\Delta T \tag{3}$$

where ρ is the density of air at atmospheric pressure, c is the specific heat of air at the atmospheric pressure.

The copper loss was estimated by measuring the root-mean-square value of the ac current flow through the heating coil and by utilizing the ac resistance of the heating coil without the heating object, which was measured in advance of the experiment by excluding the heating object from the induction heating system. (Hence, this ac resistance includes the eddy current loss in the stainless steel case because the ac resistance measurement of the heating coil was conducted including the case.) If I_{ac} and R_{ac} denote the root-mean-square ac current of the heating coil and the heating coil ac resistance without the heating object at the operating frequency, the copper loss per second P_{copper} was estimated as

$$P_{copper} = R_{ac} I_{ac}^2 \tag{4}$$

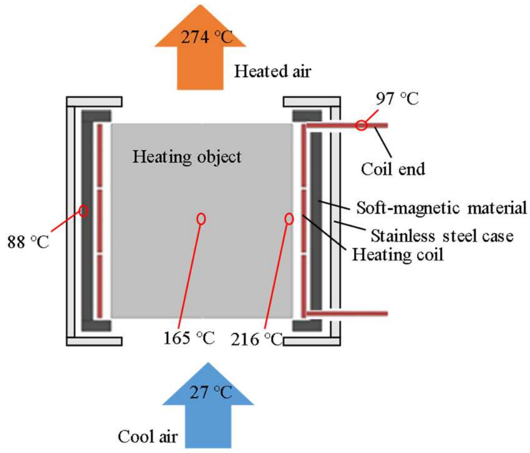

Fig. 11. Measurement points and results of temperature in prototype of proposed heating coil structure. Temperature was observed immediately after ac current of 160 Arms at 400 kHz was applied to heating coil for 3 minutes. Heating coil, soft-magnetic material, and stainless steel case were thermally isolated each from others using glasswool.

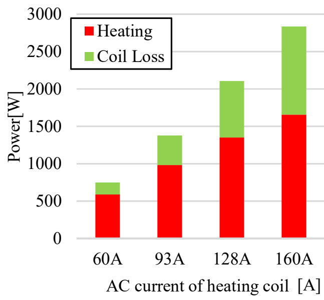

Fig. 12. Estimation result of heat generation and coil loss of prototype of proposed heating coil structure.

This experiment exhibited successful heating of the airflow. Figure 11 shows the temperature observed in the heating coil, heating object, and airflow before and after passing through the heating object, when the ac current of 160 Arms at 400 kHz flowed through the heating coil for 3 minutes. The result revealed that the temperature of the heating object was close to the airflow temperature after passing the heating object, indicating that the air was heated by the heat exchange with the heating object. The heating object appeared to be heated by the induction heating rather than the thermal conduction from the heating coil, as the temperature of the heating coil end was far smaller than that of the heating object.

Figure 12 shows the estimation results of the heat generation and the coil loss. The prototype exhibited good heating efficiency at the small heating coil current. However, the efficiency degraded at a large heating coil current. The reason is still unclear. However, the local magnetic saturation may have occurred in the prototype at a large heating coil current, to decrease the heat generation, as the dependence of the heat generation on the heating coil current was smaller than the proportionality to the square of the coil current.

The estimated copper loss was found to be far greater than the simulation. In the simulation, the loss of the proposed coil was 435 W when the operating current was set at 259 Arms at the frequency of 500 kHz. However, the estimated copper loss of the experiment was approximately 1.2 kW when the operating current is 160 Arms at the frequency of 400 kHz.

We are currently investigating the exact reason for this great copper loss increase. However, a reasonable explanation may lie in the eddy current induction in the stainless steel case. As can be seen in Fig. 5, i.e. the simulation results, the proposed heating coil structure has small magnetic field on the outer periphery of the soft-magnetic material covering the backside of the heating coil, which is effective to suppress the eddy current induction in the stainless steel case. Nonetheless, the two ends of the heating coil need to pass through the holes made on the stainless steel case to connect to the transformer secondary winding and the resonant capacitor. Therefore, the ac current flowing in these coil ends, passing through the holes, may have inducted significant eddy current in the case, thus deteriorating the heating efficiency. Consequently, this problem needs to be solved for practical application and will be addressed in our future research.

VI. Conclusions

The solenoidal heating coil is one of the most typical coil structures for the induction heating of the cylindrical heating object. However, the conventional heating coil structure of a bare solenoid coil of round- or square-shaped wire suffers from insufficient magnetic field generation inside the heating object and large copper loss of the heating coil, both of which reduce the heating efficiency. To overcome these difficulties, this paper proposed a novel heating coil structure. The proposed heating coil structure has 1. the solenoid coil of the flat rectangular wire, 2. a soft-magnetic material covering the coil edges, and 3. a soft-magnetic material covering the outer periphery of the coil. The simulation has proven the effectiveness of the proposed structure for improving heating efficiency. Currently, the proposed structure was tested experimentally, although the prototype exhibited greater power loss than the simulation. A probable reason is the eddy current induction in the stainless steel case incorporating the heating coil due to the two heating coil ends passing through the holes on the case. The solution to this problem will be addressed in future research.

References

[1] M. Fabbri, M. Forzan, S. Lupi, A. Morandi, P. L. Ribani, "Experimental and numerical analysis of DC induction heating of aluminum billets," vol. 45, no. 1, pp. 192-200, Jan. 2009.

[2] T. Lubin, D. Netter, J. Leveque and A. Rezzoug, "Induction heating of aluminum billets subjected to a strong rotating magnetic field produced by superconducting windings," *IEEE Trans. Magn.*, vol. 45, no. 5, pp. 2118-2127, May 2009.

[3] S. Choi, C. Lee, I. Kim, J. H. Jung and D. H. Seo, "Comparison on current source rectifier and inverter topologies of induction heating power supply for forging applications," 2017 20th Intl. Conf. Elect. Mach. Syst., 2017, pp. 1-6.

[4] T. Shijo, S. Kurachi, Y. Uchino, Y. Noda, H. Yamada and T. Tanaka, "High-frequency induction heating for small-foreign-metal particle detection using 400 kHz SiC-MOSFETs inverter," 2017 IEEE Energy Conversion Congr. Expos., 2017, pp. 5133-5138.

[5] D. Paesa, C. Franco, S. Llorente, G. Lopez-Nicolas and C. Sagues, "Adaptive Simmering Control for Domestic Induction Cookers," IEEE Trans. Ind. Appl., vol. 47, no. 5, pp. 2257-2267, Sept.-Oct. 2011.

[6] L. C. Meng, K. W. E. Cheng and S. L. Ho, "Multicoils Design for Induction Cookers With Applying Switched Exciting Method," IEEE Trans. Magn., vol. 48, no. 11, pp. 4503-4506, Nov. 2012.

[7] W. Han, K. T. Chau and Z. Zhang, "Flexible induction heating using magnetic resonant coupling," IEEE Trans. Ind. Electron., vol. 64, no. 3, pp. 1982-1992, Mar. 2017.

[8] M. Hataya, K. Kamaeguchi, E. Hiraki, K. Umetani, T. Hirokawa, M. Imai, and S. Sadakata, "Verification fo the reduction of the copper loss by the thin coil structure for induction cookers," in Proc. IEEE Intl. Power Electron. Conf. (IPEC2018), Niigata, Japan, May 2018, pp. 410-415.

[9] K. Kamaeguchi, K. Umetani, and E. Hiraki, "Axial heating coil structure for reducing magnetic levitation force of all-metal type induction cookers," in Proc. IEEE Intl. Conf. Renewable Energy Research Appl. (ICRERA2019), Nov. 2019, Brasov, Romania, pp. 1-7.

[10] H. Kurose, D. Miyagi, N. Takahashi, N. Uchida, and K. Kawanaka, "3-D eddy current analysis of induction heating appratus considering heat emission, heat conduction, and temperature dependence on magnetic characteristics," IEEE Trans. Magn., vol. 45, no. 3, pp. 1847-1850, Mar. 2009.

[11] H. Kagimoto, D. Miyagi, N. Takahashi, N. Uchida, and K. Kawanaka, "Effect of temperature depnedence of magnetic properties on heating characteristics of induction heater," IEEE Trans. Magn., vol. 46, no. 8, pp. 3018-3021, Aug. 2010.

[12] H. Tsuboi, K. Ikeda, and M. Kurata, "Eddy current analysis for the pipe welding," IEEE Trans. Magn., vol. 34, no. 4,pp. 1234-1236, Jul. 1998.

[13] F. Dughiero, M. Forzan, C. Pozza, and E. Sieni, "A translational coupled electromagentic and thermal innovative model for induction welding of tubes," IEEE Trans. Magn., vol. 48, no. 2pp. 483-486, Feb. 2012.

[14] R. Crawford and J. Douglas, "Catalytic converter structures with induction heating," U.S. Patent US20150075137 A1, Mar 19, 2015.

[15] N. Leahey, R. Crawford, J. Douglas, and J. Baumann, "Induction heating of catalytic converter systems and its effect on diesel exhaust emissions during cold start," SAE Technical Paper 2018-01-0327, 2018.

[16] S. E. Schwarz, "Electrodynanics," in Electromagnetics for engineers, Orland, FL, USA: Sounders Colledge Publishing, 1990, pp. 214-246.

[17] M. Hataya, Y. Oka, K. Umetani, E. Hiraki, T. Hirokawa, and M. Imai, "Novel thin heating coil structure with reduced copper loss for high frequency induction cookers," in Proc. IEEE Intl. Conf. Elect. Mach. Syst. (ICEMS2016), Chiba, Japan, Nov. 2016, pp. 1–6.

[18] K. Umetani, "Improvement of saturation property of iron powder core by flux homogenizing structure," IEEJ Trans. Elect. Electron. Eng., vol. 8, no. 6, pp. 640-648, Sep. 2013.

[19] K. Umetani, Y. Itoh, and M. Yamamoto, "A detection method of DC magnetization utilizing local inhomogeneity of flux distribution in power transformer core," in Proc. IEEE Energy Conversion Congr. Expo., Pittsburgh, PA, 2014, pp. 3739-3746.